CITATION: X. Qu, H. Zhang, H. Kong, D. Chen, Z. Yang, E. Mäkilä, J. Salonen, H. A. Santos, M. Hai, D. A. Weitz, Porous Silicon Nanoparticles Conjugated Magnetite-Chitosan Graphene Oxide Nanoparticles for Effective Removal of Complex Pollutants. *Adv. Sustainable Syst.* 2024, 2300471. https://doi.org/10.1002/adsu.202300471

DOI https://doi.org/10.1002/adsu.202300471

RESEARCH ARTICLE

ADVANCED SUSTAINABLE SYSTEMS
www.advsustainsys.com

Porous Silicon Nanoparticles Conjugated Magnetite-Chitosan Graphene Oxide Nanoparticles for Effective Removal of Complex Pollutants

Xiangmeng Qu, Hongbo Zhang, Haixin Kong, Dong Chen, Zhou Yang, Ermei Mäkilä, Jarno Salonen, Hélder A. Santos, Mingtan Hai, and David A. Weitz**

The effective removal of complex pollutants is extremely challenging for environmental and material science, especially pollutants including detergents and pesticides do not decompose or degrade in the aquatic environment which cannot be easily removed. Here, a novel biocompatible superparamagnetic nanocomposite integrating the advantages of porous silicon nanoparticles is developed, the chelation ability of chitosan, and graphene-oxide-iron that can simultaneously adsorb complex hydrophobic and hydrophilic pollutants on their internal and external surfaces which have significantly improved pollutant removal efficiency over the current existing methods. A porous silicon nanoparticle (PSi) conjugated magnetite-chitosan-reduced graphene oxide (MCRGO) nanoparticles (PSi-MCRGO) are synthesized for complete removal of detergent, pesticide, and toxic heavy metals cadmium and lead ions from water at a favorable room temperature. The adsorption behavior of the nanocomposites fits well with the Freundlich isotherm and pseudo-second-order kinetics model by adsorption mechanism. Moreover, the fresh and recycled nanocomposites are easily separated by an external magnetic field for reusability due to super magnetite response and show high binding capacity for toxic heavy metal ions. Furthermore, the nanocomposites are biocompatible and reusable, and for the fourth time, recycled nanocomposites can completely remove toxic heavy metals. Overall, the novel nanocomposites completely remove complex pollutants which hold great potential for real water treatment.

1. Introduction

In the 2015 UN Sustainable Development Summit,[1] “Clean Water and Sanitation” has been set as an urgent global sustainable development goal (SDG) for 2030. The primary toxic heavy metals present in water and soils, including lead and cadmium, are very dangerous to human health and ecosystems.[2,3] Exposure to heavy metals leads to the development of various types of cancer, kidney damage, and even death in some cases.[4,5] The non-essential heavy metals include cadmium, lead, copper, mercury, arsenic, etc. Lead (II) and cadmium (II) are metals that appear together in many samples. Lead is highly harmful to live organisms even in very low concentrations which can induce severe neurological and physiological repercussions.[6] The harmful effects of cadmium include several acute and chronic disorders, renal damage, hypertension, and testicular atrophy.[7] The simultaneous removal of both lead and cadmium is imperative. Sodium dodecyl sulfate (SDS: $C_{12}H_{25}SO_4Na$) and related surfactants[8] are broadly used in

---

X. Qu[+], H. Zhang, H. Kong[++], Z. Yang, M. Hai
School of Materials Science and Engineering
University of Science and Technology Beijing
Beijing 100083, P. R. China
E-mail: mhai@seas.harvard.edu

The ORCID identification number(s) for the author(s) of this article can be found under https://doi.org/10.1002/adsu.202300471

[+]Present address: School of Biomedical Engineering, Sun Yat-Sen University, Guangzhou Higher Education Mega Center, Guangzhou 510006, P. R. China

[++]Present address: Durham University, South Road, Durham DH1 3LG, United Kingdom

[+++]Present address: College of Chemical and Biological Engineering, Zhejiang University, No. 38 Zheda Road, Hangzhou 310027, P. R. China

DOI: 10.1002/adsu.202300471

X. Qu[+], H. Zhang, H. Kong[++], D. Chen[+++], M. Hai, D. A. Weitz
Harvard John A. Paulson School of Engineering and Applied Sciences
Harvard University
Cambridge, MA 02138, USA
E-mail: weitz@seas.harvard.edu

H. Zhang
Department of Pharmaceutical Sciences Laboratory
Åbo Akademi University
Turku FI-20520, Finland

H. Zhang
Turku Center for Biotechnology
University of Turku and Åbo Akademi University
Turku FI-20520, Finland

E. Mäkilä, J. Salonen
Laboratory of Industrial Physics
Department of Physics
University of Turku
Turku FI-20014, Finland

multiple applications, including everyday life for laundry, for lysing cells during DNA extraction, for unraveling proteins in SDS-PAGE (Polyacrylamide Gels) in research labs, and much more. SDS has very good water solubility, thus it is very difficult to remove from water. Water pollution with detergents containing mainly anionic SDS can be toxic to ecosystems and humans and cause several diseases.[9] SDS does not decompose or degrade in an aquatic system. The accumulation of detergents in water represents a serious environmental problem. The removal of the detergent SDS and heavy metals simultaneously from water is very important from an environmental point of view.[9]

The conventional methods for heavy metals removal include membrane techniques, chemical precipitation, coagulation and flocculation, ion exchange or chelation, and adsorption by activated carbon.[10–13] However, these methods have several issues to address including incomplete metal removal, high capital and operational costs, or problems with the disposal of the residual metal sludge. Adsorption is considered an effective and economical method for pollutant removal from water due to easy handling. For example, magnetite-based materials including nano-magnetite, are very effective in the removal of heavy metal ions.[14] However, these adsorbents are difficult to use in a continuous flow system due to small particle size and instability.[14] On the other hand, graphene-based materials, including graphene[15] and graphene oxide,[16] have shown many applications in composite materials and devices[17] to overcome this difficulty. Chitosan is a natural biopolymer[18–19] with the unique ability to chelate dissolved metals in water with its multiple binding sites along the polymer chain and has been recognized as an effective new adsorbent for heavy metal arsenic ions. Positively charged magnetite-reduced graphene oxide chitosan microsphere is useful for As (III) removal,[20] but cannot be used for heavy metal cationic ions including copper, cadmium, and lead removal due to extremely low removal efficacy. Moreover, the use of cheap biocompatible materials as potential adsorbents and the processes developed based on exploring natural adsorbents that can improve cost-effectiveness have been a hot research area in recent years.[20–24] It is still a major challenge to develop simple and efficient adsorbents to enhance adsorption capacity at low cost.

Taking advantage of the large surface area and stability of the reduced graphene oxide (rGO) as well as the chelation ability of chitosan, we synthesized negatively charged magnetite-chitosan reduced graphene oxide (MCRGO) nanohybrids, which can efficiently remove heavy metals or positively charged materials. In addition, porous materials (such as porous silicon nanoparticles and microparticles (PSi NPs and MPs)) with amine surface group have unique properties such as large surface area, high surface-to-volume ratio, and flexible surface modification,[25–28] which have potential for the simultaneous adsorption of different hydrophobic and hydrophilic pollutants other than heavy metals in water and soil. The carboxyl (COOH) surface group of MCRGO activated by *N*-(3-Dimethylaminopropyl)-*N*′-ethylcarbodiimide hydrochloride (EDC) can easily react with the amine group of PSi NPs to fabricate PSi conjugated MCRGO nanohybrids. Therefore, we have fabricated a novel MCRGO nanocomposite with a COOH surface group at a low temperature (338 K) and then conjugated the MCRGO with PSi NPs and MPs through a chemical reaction at 298 K for the simultaneous removal and separation of heavy metals such as lead and cadmium, as well as the anionic detergent SDS and pesticide, from water. The magnetic nanoparticles enable the easy separation of the nanocomposites for recycling by an external magnetic field to low cost and increase removal efficiency and reusability. The removal efficiency of positively charged heavy metals Cd^{2+} and lead Pb^{2+} as well as the negatively charged $C_{12}H_{25}SO_4^-$ by the nanocomposites of PSi-MCRGO are evaluated. The adsorption kinetics of the heavy metals is investigated. The removal efficiency of pesticides by the PSi-MCRGO nanocomposites and the removal of the heavy metals by the recycled PSi-MCRGO nanocomposites is also performed. The biocompatibility and reusability of the nanocomposites are investigated.

To achieve the United Nation's Sustainable Development Goals of Clean Water and Sanitation, we develop novel environmental-friendly superparamagnetic nanomaterials for the complete removal of complex pollutants including heavy metals, detergents, and pesticides from water. The biocompatible nanomaterials integrating the advantages of porous silicon nanoparticles, and the chelation ability of chitosan and graphene-oxide-iron can simultaneously adsorb hydrophobic and hydrophilic pollutants on their internal and external surfaces. The adsorption behavior of the nanocomposites fits well with the Freundlich isotherm and the pseudo-second-order kinetics model by adsorption mechanism at favorable room temperature. The supermagnetic response nanomaterials can be separated easily by an external magnetic field for reusability as low-cost adsorbents. Fresh and recycled biocompatible nanomaterials can completely remove complex pollutants and have significantly improved pollutant removal efficiency over the currently existing methods for water treatment applications. These positive results indicate that further research on these pollutant-binding superparamagnetic nanomaterials will help achieve the SDGs of CLEAN WATER AND SANITATION for human beings on land, animals on land, and below water.

2. Results and Discussion

For the simultaneous complete removal of heavy metal ions and other pollutants including detergents and pesticides from water, we fabricate negatively charged magnetic recyclable magnetite-chitosan-reduced graphene oxide (MCRGO) and porous silicon nanoparticles conjugated MCRGO (PSi-MCRGO) nanocomposites (**Scheme 1**).

To prepare MCRGO and PSi-MCRGO nanoparticles, we first synthesize single-layer graphene oxide (GO). The morphology of the synthesized GO is confirmed by scanning electron microscopy (SEM) and atomic force microscopy (AFM) (**Figure 1a**; Figure S1a–c, Supporting Information). The AFM result confirms the presence of a single layer of GO, and the size of GO is ≈100 nm. This can be seen by the corresponding height profile in Figure S1d (Supporting Information) which demonstrates that GO is fully exfoliated with a thickness of ≈1 nm. The oxidation

---

H. A. Santos
Department of Biomedical Engineering and W.J. Kolff Institute for Biomedical Engineering and Materials Science University of Groningen/University Medical Center Groningen Ant. Deusinglaan 1
Groningen 9713 AV, The Netherlands

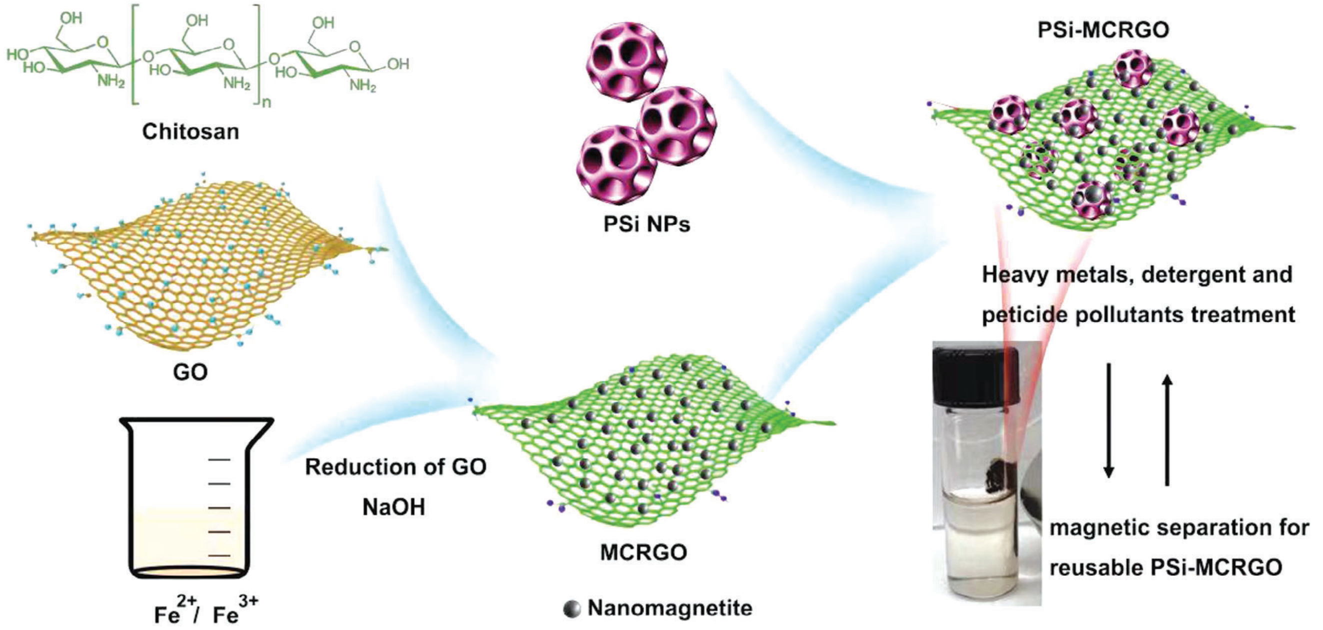

Scheme 1. The chemical synthesis of magnetic recyclable PSi-MCRGO nanocomposites and their applications in heavy metals, detergents, and pesticides pollutants removal treatment.

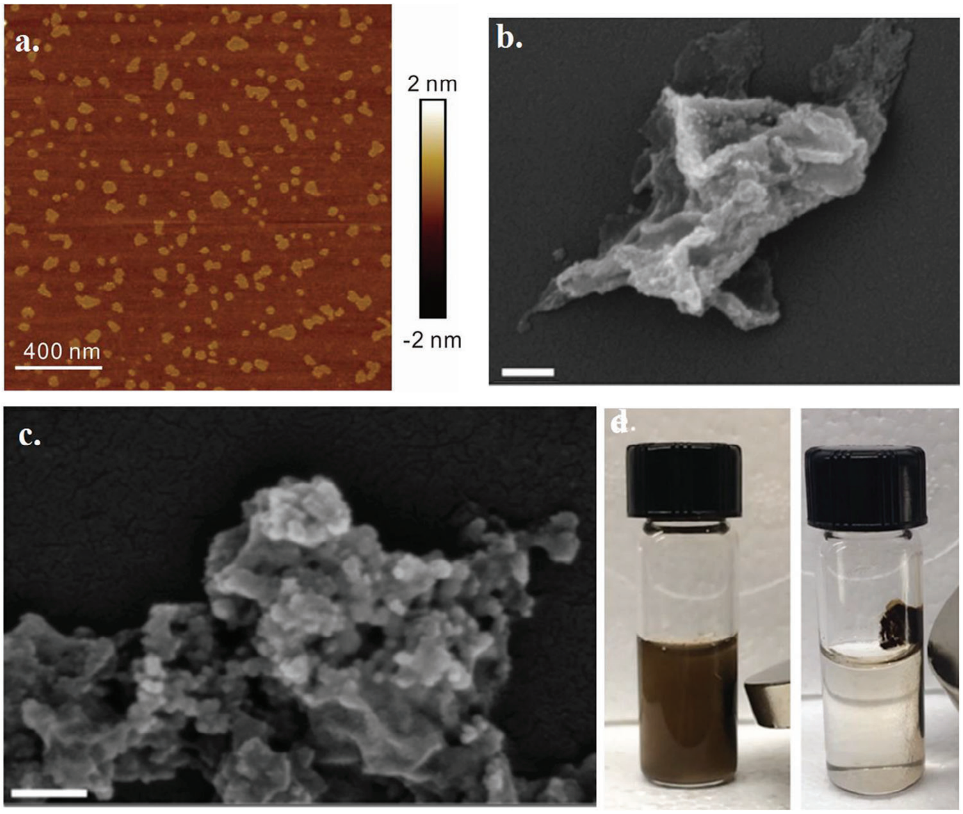

Figure 1. SEM image of the synthesized PSi-MCRGO and magnetic response of PSi-MCRGO. a) AFM image of GO. The scale bar denotes 400 nm. b) SEM image of MCRGO. The scale bar denotes 100 nm. c) SEM image of PSi-MCRGO. The scale bar denotes 100 nm. d) Magnetic response of PSi-MCRGO particles.

process generates a C/O atomic ratio of 2.26:1 for the synthesized GO, as indicated by the X-ray photoelectron spectroscopy (XPS) survey spectrum in Figure S1e (Supporting Information). Two oxygenic species, including the C—O bond and C═O bond, contributed 52% of the total area (Figure S1f, Supporting Information) under the C1s peak in Figure S1e (Supporting Information).

Following the production of the single-layer GO, we synthesize magnetite-reduced graphene oxide (MRGO) and magnetite-chitosan-reduced graphene oxide (MCRGO) particles by the chemical reduction reaction via NaOH solutions at 338 K under nitrogen protection. The morphology of MCRGO particles is imaged by SEM with a hydrodynamic diameter ≈400 nm (Figure 1b). The addition of the biopolymer chitosan and magnetic nanoparticles is hypothesized to enhance the adsorption ability of the MRGO particles due to the abundant binding sites available for metal chelation and the easy removal of the particles from water by the magnetic field, respectively. The porous silicon nanoparticles (PSi NPs) and macroparticles (PSi MPs) with an amine surface group can easily conjugate with the COOH surface group of MCRGO through a one-step chemical reaction at room temperature. The COOH surface group of MCRGO is first activated by EDC for half an hour at 298 K, then reacted with the amine group of PSi NPs to form amides for 24 h under magnetic stirring at 298 K. The SEM image of PSi-MCRGO nanocomposites is shown in Figure 1c. The magnetic response of PSi-MCRGO to the external magnetic field is tested for the separation of the synthesized nanomaterials (Figure 1d).

XPS spectra of the synthesized MRGO, MCRGO, and PSi-MCRGO particles show that the C/O atomic ratio is decreased due to the reduction of GO to RGO (Figure S2, Supporting Information). The wide scan XPS spectrum of the MCRGO shows the photoelectron lines attributed to C1s, N1s, O1s, and Fe2p, respectively. The peak of Fe2p was located at 711.8 eV and is indicative of the formation of the magnetite (γ-Fe_3O_4) in the RGO matrix. The peak of O1s is located at 531.93 eV, indicating that the oxygen-containing functional groups are mainly from chitosan and GO sheets (Figure S2, Supporting Information). The X-ray photoelectron spectroscopy (XPS) spectrum (Figure S2c, Supporting Information) confirms the successful reaction of porous silicon nanoparticles conjugated MCRGO with Fe, C, O, Si, and N peaks.

The Specific Surface Area (SSA) is a dominant parameter that measures a solid material's surface per unit of volume or mass, revealing how porous or fine-grained it is. High SSA materials, like catalysts or adsorbents, have more surface for reactions or binding. The specific surface areas (SSA) obtained for the MCRGO and PSi-MCRGO nanocomposites by the Brunauer-Emmett-Teller (BET) method are 89.0 ± 1.0 and 102.1 ± 1.3 $m^2\ g^{-1}$, respectively. According to dynamic light scattering (DLS) and electrophoretic mobility measurements, the hydrodynamic diameter of the MCRGO is ≈400 nm, and the zeta potential is -21.3 ± 0.4 mV. The hydrodynamic diameter of the PSi-MCRGO is ≈450 nm, while the surface zeta potential is -9.7 ± 0.3 mV. These results indicate that the negatively charged MCRGO and PSi-MCRGO particles appear to have enough available surface area and suitable surface charge for the adsorption of positively charged metal ions through electrostatic attraction.

The magnetic characterization of the synthesized MCRGO and PSi-MCRGO nanocomposites has been performed through the magnetic hysteresis curve study (Figure S3, Supporting Information). The results show that both MCRGO and PSi-MCRGO nanocomposites are superparamagnetic with a high concentration of magnetite at room temperature which is desirable for many practical applications in the field of magnetic separation. The super magnetic response property enables the easy removal of the PSi-MCRGO after heavy metals adsorption through an application of an external magnetic field. The magnetic separation of PSi-MCRGO from aqueous solution by an external magnetic field is shown in Figure 1d and Video S1 (Supporting Information). The separation is almost completed within 1 min at room temperature.

The positively charged hydrophilic PSi NPs have a great capability for loading hydrophobic payloads.[25,26] The novel magnetic PSi-MCRGO nanocomposites combine the advantages of PSi NPs, chitosan, and MCRGO are efficient adsorbents for complex pollutants removal. As a result, the PSi-MCRGO is negatively charged when the MCRGO concentration is higher than the concentration of PSi NPs. For the simultaneous removal of Cd^{2+} and Pb^{2+}, as well as other heavy metal ions from water, the PSi-MCRGO is more effective when the nanocomposite is negatively charged due to the electrostatic interactions between the metal ions and the MCRGO. and the PSi-MCRGO composites are almost as effective as MCRGO (**Figure 2**a,b). The comparison of the lead and cadmium removal efficiency from water containing 4 mg L^{-1} Cd^{2+} and 7 mg L^{-1} Pb^{2+} by MCRGO and PSi-MCRGO adsorption is investigated at 298 K (Figure 2). Although the PSi NPs have high surface area and porosity, the Pd^{2+} and Cd^{2+} removal efficiencies are low due to the electrostatic repulsion. In addition, the PSi NPs also slightly reduce the Pd^{2+} and Cd^{2+} removal efficiency of MCRGO, which is probably due to the electrostatic charge neutralization of MCRGO hybrids.

Besides heavy metals, there are also many other types of pollutants in the water, for example, synthetic chemicals including negatively charged hydrophilic detergent pollutants and important organic pollutant pesticides. Here, the anionic surfactant sodium dodecyl sulfate (SDS) is chosen as an example for demonstrating the absorption ability of PSi NPs and PSi-MCRGO composites. The anionic $C_{12}H_{25}SO_4^-$ removal from water by MCRGO or PSi NPs or PSi-MCRGO is investigated at 298 K. The removal efficiency of $C_{12}H_{25}SO_4^-$ from detergent water solutions by negatively charged MCRGO hybrids is less than 5% mainly due to the electrostatic repulsion and strong adsorption of Na^+ to the MCRGO from the SDS, but for PSi NPs and PSi-MCRGO, the removal efficiency is over 90% when the SDS concentration is below 5 mg mL^{-1} (Figure 2c). The pesticide removal efficiency study by MCRGO or PSi NPs or PSi-MCRGO is also carried out at 298 K after adsorption for 2 h at 298 K. The removal efficiency of pesticides by MCRGO and PSi-MCRGO is over 90% when the pesticide concentration is below 5 µg mL^{-1} (Figure 2d). The PSi-MCRGO can simultaneously eliminate cationic heavy metal ions and anionic surfactants from water and organic pesticides as well. Our novel magnetic functional nanocomposites PSi-MCRGO could deal with complex pollutants simultaneously that do not decompose or degrade in the aquatic environment and show great potential for real water treatment.

To find an optimized platform for polluted water treatment, we have compared different platforms by conducting heavy metal removal experiments. At the same concentration, MCRGO clearly

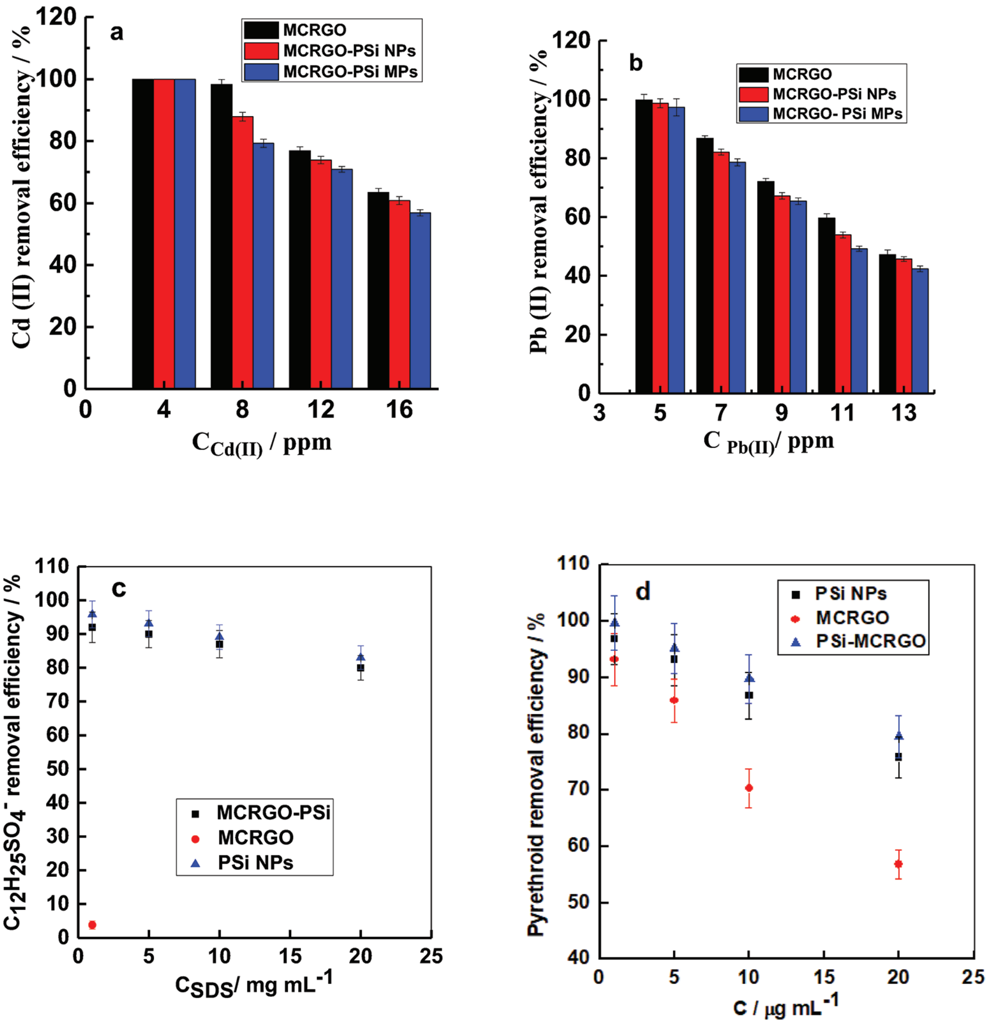

Figure 2. The simultaneous removal of heavy metals, SDS, and pesticide study. Lead a) and cadmium b) removal efficiency from water at different concentrations [4 mg L^{-1} Cd^{2+} + 5 mg L^{-1} Pb^{2+}; 4 mg L^{-1} Cd^{2+} + 7 mg L^{-1} Pb^{2+}; 8 mg L^{-1} Cd^{2+} + 9 mg L^{-1} Pb^{2+}; 12 mg L^{-1} Cd^{2+} + 11 mg L^{-1} Pb^{2+}; 16 mg L^{-1} ppm Cd^{2+} + 13 mg L^{-1} Pb^{2+}] by 2 mg MCRGO hybrids and PSi-MCRGO or PSi MPs for 1 h adsorption from 10 mL water solution. c) The $C_{12}H_{25}SO_4^-$ removal efficiency from various SDS water solutions and pesticide removal efficiency by 2 mg MCRGO or PSi-MCRGO composites and 100 µg PSi NPs at 298 K. d)The pyrethroid removal efficiency by 4 mg MCRGO or PSi-MCRGO composites and 200 µg PSi NPs at 298 K.

has higher copper ion removal efficiency than that of GO and MRGO, due to the chelation properties of the chitosan (Table S1, Supporting Information). Thus, the addition of the biopolymer chitosan enhances the adsorption capacity, and thus, the MCRGO is much more efficient for heavy metals removal.

In addition, we have also compared the heavy metal removal efficiency of MCRGO and PSi-MCRGO. The results indicate that at the same concentration, the MCRGO has higher Pd^{2+} and Cd^{2+} removal efficiency in comparison to the PSi-MCRGO (Figure S4, Supporting Information). This is probably due to the surface charge of PSi-MCRGO (−9.7 mV), far less than −21 mV of MCRGO. The stronger electrostatic interaction between the MCRGO and the positively charged heavy metal ions makes them a little bit better composites for heavy metals removal treatment than that of PSi-MCRGO.

We have also evaluated the effect of the size of PSi on the heavy metal removal efficiency. We conducted the heavy metals Cd^{2+} and Pb^{2+} removal experiment by using different MCRGO conjugated with both PSi NPs and PSi MPs. The PSi NPs are ≈160 nm in size with surface areas of 219 m^2 g^{-1} and PSi MPs are ≈15 µm in size with surface areas of 205 m^2 g^{-1}. The lead and cadmium removal efficiencies from water at different concentrations by MCRGO; MCRGO-PSi NPs and MCRGO-PSi MPs suspension (the volume ratio between water and absorbent was 5:1) at 298 K, are shown in **Figure 3**a. The concentration difference between Pb^{2+} and Cd^{2+} led to easy separation of the maximum UV peak. The MCRGO-PSi NP nanocomposites lead to higher removal efficiency than that of the MCRGO-PSi MPs at the same concentration.

The adsorption isotherm could provide information about the adsorption mechanism, surface property, and the affinity of an adsorbent to an adsorbate at a given temperature under equilibrium conditions. The adsorption isotherms of Cd^{2+} and Pb^{2+} for MCRGO and PSi-MCRGO are shown in Figure 3. The lead and

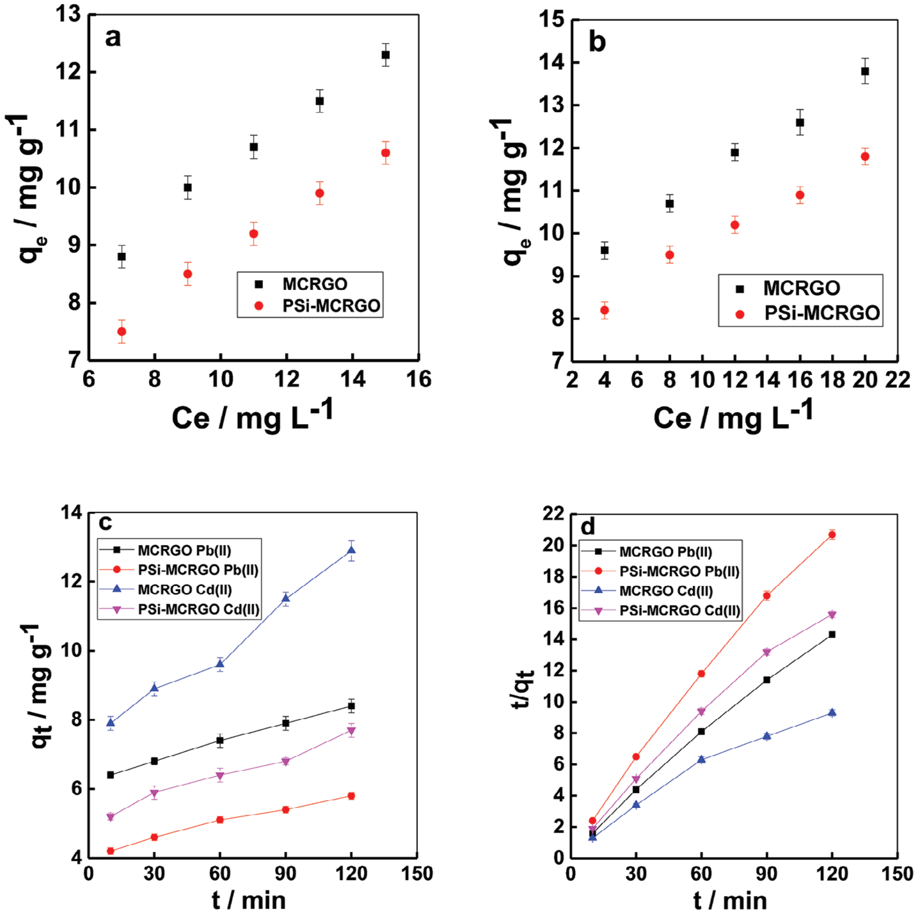

Figure 3. Adsorption isotherms and kinetic adsorption study. a) Pb^{2+} and b) Cd^{2+} from water after 1 h adsorption on the MCRGO and PSi-MCRGO composites at 298 K. c) the heavy metals lead and cadmium removal rate versus adsorption time by MCRGO and PSi-MCRGO hybrids. d) Transformed rate plot t/q_t versus t.

cadmium concentrations vary from 4 to 20 mg L^{-1}, and the adsorption data are fitted with the Freundlich isotherm model with Equation (1)[29]:

$$q_e = k(Ce)^{1/n} \tag{1}$$

where q_e is the amount of lead or cadmium adsorbed unit weight of adsorbent (mg g^{-1}); Ce is the equilibrium concentration of lead or cadmium (mg L^{-1}); k is indicative of the relative adsorption capacity of the adsorbent (mg g^{-1}), and $(1/n)$ is the adsorption intensity. All Freundlich isotherm parameters are obtained through the nonlinear fitting, and the adsorption data fit Freundlich isotherms well as R^2 is larger than 0.98 as shown in Table S2 (Supporting Information). The Freundlich constant n is found to be greater than 1 which indicates a favorable condition for adsorption. The n values for lead and cadmium by MCRGO and PSi-MCRGO composites are all larger than 2 which shows more favorable conditions for adsorption. The maximum adsorption capacity for lead and cadmium by MCRGO hybrids at 0.2 mg mL^{-1} concentration is shown in (Figure S5, Supporting Information). The removal capacity of cadmium is higher than that of lead with MCRGO. The removal of lead and cadmium with MCRGO is higher than that with PSi-MCRGO.

The kinetic of heavy metal ions removal has been determined to understand the adsorption behavior of the nanocomposites. The kinetic data for the adsorbent of lead and cadmium to MCRGO and PSi-MCRGO is also fitted to a pseudo-second-order kinetic model,[30,31] and the kinetic rate equation is represented by Equation (2):

$$\frac{dq_t}{dt} = k_2 \times \left(q_e - q_t\right)^2 \tag{2}$$

where, q_e and q_t represent the sorption capacity at equilibrium and the solid phase loading of lead or cadmium at time t, respectively; k_2 represents an adsorption rate constant of pseudo-second order[30,31] with the unit of mg g^{-1}.min^{-1}. The following linear equation can also be obtained by integrating Equation (2) with the boundary conditions (Equations 3 and 4):

$$\frac{t}{q_t} = \frac{1}{k_2 q_e^2} + \frac{t}{q_t} \tag{3}$$

$$V_0 = k_2 q_e^2 \tag{4}$$

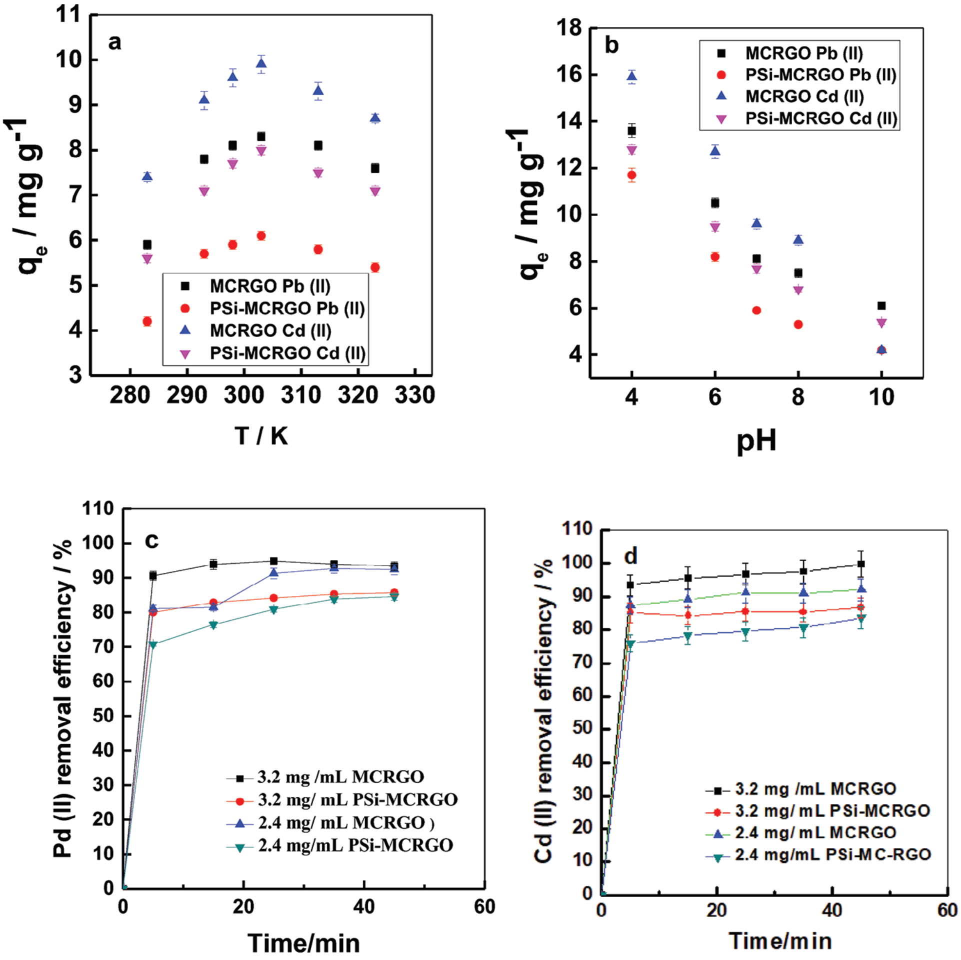

Figure 4. Effect of the temperature a) and pH value b) on Pb^{2+} (7 mg L^{-1}) and Cd^{2+} (8 mg L^{-1}) adsorption from water after 1 h adsorption with 0.1 mg mL^{-1} MCRGO and PSi-MCRGO. c,d) Kinetic study of lead and cadmium ion adsorption by MCRGO and PSi-MCRGO. The adsorption of 7 mg L^{-1} lead and 8 mg L^{-1} cadmium solution at pH 7.0 for 1 h adsorption with 0.1 mg mL^{-1} MCRGO and PSi-MCRGO at 298 K.

where, V_0 (mg g^{-1}.min^{-1}) is the initial sorption rate which can be determined by plotting the t/q_t versus t (Figure 3c,d). Good fits for all concentrations are found with R^2 larger than 0.98. The experimental results listed in Table S3 (Supporting Information) indicate that lead and cadmium absorption onto MCRGO and PSi-MCRGO is favorable according to the pseudo-second-order kinetics model.

To demonstrate the temperature effect on lead and cadmium removal from water, we have fixed the experimental conditions to 0.1 mg mL^{-1} of MCRGO and PSi-MCRGO at pH 7.0 for the adsorption of 7 mg L^{-1} of lead and 8 mg L^{-1} of cadmium from water with an adsorption time of 1 h, at temperatures ranging from 283 to 323 K. The equilibrium adsorption decreases with increasing temperature. The temperature of the maximum lead and cadmium adsorption by MCRGO and PSi-MCRGO is ca. 298–308 K, which confirms a favorable room temperature adsorption process of lead and cadmium onto the PSi-MCRGO (**Figure** 4a).

To demonstrate the pH effect on lead and cadmium removal from water, we have fixed the experimental conditions to 0.1 mg mL^{-1} of MCRGO and PSi-MCRGO at 298 K for the adsorption of 7 mg L^{-1} of lead and 8 mg L^{-1} of cadmium from water with an adsorption time of 1 h, at different pH value ranging from 4 to 10. The pH effect on the heavy metals lead and cadmium adsorption by MCRGO and PSi-MCRGO is shown in Figure 4b. Positive charged heavy metal lead and cadmium ions removal on the negatively charged MCRGO and PSi-MCRGO surface is mainly through electrostatic interaction. Under most pH conditions, lead and cadmium ions are present in a positive form Pb^{2+} and Cd^{2+}. The pH value dependence of both lead and cadmium adsorption onto the surface of MCRGO and PSi-MCRGO can be explained by the point of zero charge (pH_{PZC}) of the adsorbent. At pH smaller than pH_{PZC}, the MCRGO and PSi-MCRGO surface is negatively charged, it attracts positively charged heavy metals lead and cadmium ions, resulting in large adsorption at a low pH value. The value of adsorption capacity q_e becomes large at low pH for lead and cadmium removal. At pH is larger than pH_{PZC}, as the pH value increases, the negatively charged surface sites of MCRGO and PSi-MCRGO decrease, causing a reduction in positive charged heavy metals lead and cadmium adsorption. The value of q_e becomes small at high pH for lead and cadmium removal, but it is still larger than 4. The strong adsorption of lead and cadmium ions by MCRGO and PSi-MCRGO at higher pH

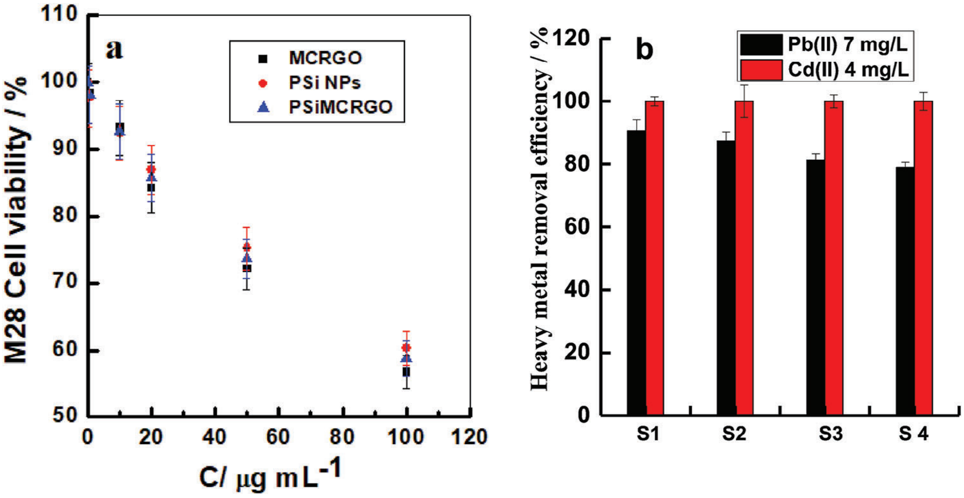

Figure 5. The biocompatibility study of MCRGO, PSi NPs, and PSi-MCRGO on M28 cell viability after 24 h incubation at 310 K a) and b) the removal efficiency of the toxic heavy metal ions by the recycled MCRGO and PSi-MCRGO hybrids at different amounts. (S1: 0.2 mg MCRGO; S2: 0.2 mg PSi-MCRGO; S3: 0.1 mg MCRGO; S4: 0.1 mg PSi-MCRGO for the simultaneous removal of 4 mg L^{-1} Cd (II) and 7 mg L^{-1} Pb (II) from 1 mL water solution).

values indicates that the adsorption process is followed by surface complexation, rather than electrostatic interactions maybe due to the unique property of chitosan and porous silicon nanoparticles.

The kinetic study of lead and cadmium removal by different MCRGO and PSi-MCRGO is determined to understand the adsorption behavior of the MCRGO and PSi-MCRGO. The lead and cadmium removal efficiency by MCRGO and PSi-MCRGO is investigated at different time intervals. The heavy metal ions adsorption process is very fast, almost completed within 5 min for both MCRGO and PSi-MCRGO (Figure 4c). The kinetic data for the adsorbent is different for MCRGO and PSi-MCRGO. When PSi NPs are conjugated with MCRGO, the heavy metal adsorption fluctuates from 5 to 30 min and is balanced at ≈40 min. However, PSi NPs do not affect the maximum removal efficiency as the adsorption is saturated to almost the same levels after 45 min for both MCRGO and PSi-MCRGO.

The biocompatibility of the PSi-MCRGO nanocomposites is another important issue to be addressed. The biocompatibility of PSi NPs is confirmed by our previous work.[25,26] To evaluate the safety of MCRGO and PSi-MCRGO, we do the cell viability assay of those materials toward a non-carcinoma human cell line, M28 cells. The result indicates that MCRGO and PSi-MCRGO have good biocompatibility at a concentration below 50 μg mL^{-1} on normal human cells, thus the small amount of MCRGO and PSi-MCRGO residue in water will not lead to secondary pollution in human health and environment (**Figure** 5a). Overall, these environment-friendly biomaterials hold great potential for complex water treatment.

The magnetic properties of fresh and recycled MCRGO and PSi-MCRGO are performed at 300 K. The hysteresis curve of the fresh and recycled hybrids shows that they have similar magnetic properties (Figure S3, Supporting Information). The recycled MCRGO and PSi-MCRGO are obtained by magnetic separation and further freeze-drying treatment, they are reused to simultaneously remove toxic heavy metals. The regeneration and reuse of the adsorbents is very crucial in practical applications due to the stringent ecological and economic demands for sustainability. The effective adsorbent should possess high absorption capacity and desorption properties to lower the cost. The nanocomposites can be reused several times, and the removal efficiency of heavy metals by the different rounds of nanomaterials has been performed at 298 K (Figure S6, Supporting Information). The results indicate that the fourth time recycled MCRGO and PSi-MCRGO completely remove toxic heavy metals of Pd^{2+} and Cd^{2+} when the Cd^{2+} concentration is below 4 mg L^{-1} (Figure 5b), and the synthesized nanocomposites have good reusability and great potentials for low-cost water treatment. The real concentration of Pd^{2+} and Cd^{2+} in water is generally below 1 mg L^{-1}, so we deduce that the recycled nanocomposites can eliminate the toxic heavy metals from the water solution. The fresh and recycled magnetic functional nanocomposites can effectively remove organic dye including oil red O. From all the results, we hypothesize that the biocompatible PSi-MCRGO nanocomposites are environment-friendly and economically affordable magnetic functional material for real complex water treatment.

3. Conclusion

Herein, we report the chemical fabrication of porous silicon nanoparticles conjugated MCRGO (PSi-MCRGO) as a biocompatible magnetic-recyclable functionalized nanomaterial and reusable adsorbent for different pollutants complete removal from water. The MCRGO and PSi-MCRGO nanocomposites show high binding capacity for positively charged heavy metal ions and show near-complete heavy metals Pb^{2+}, Cd^{2+}, and Cu^{2+} removal by adsorption. The addition of the biopolymer chitosan enhances the adsorption capacity and promotes removal efficiency. PSi-MCRGO is effective in the removal of anionic surfactant SDS and organic pesticides that do not decompose or degrade in the aquatic environment. The adsorption process of lead and cadmium is favorable according to the pseudo-second-order kinetics model by adsorption mechanism at room temperature. The PSi-MCRGO nanocomposites are super magnetic responsive and can be easily removed from water by a magnetic field after the water treatment, they are recyclable. The recycled PSi-MCRGO can completely remove the heavy metals after 4 cycles from water. Importantly, the PSi-MCRGO nanocomposites are shown to be biocompatible, and they are not harmful to human cells. Overall, the PSi-MCRGO is applicable for cationic heavy metals ions and anionic detergent surfactants simultaneous removal from water and pesticide removal as well by adsorption mechanism, which enables the purification of very complex polluted water. Thus, the developed environment-friendly and economically affordable magnetic functionalized nanocomposites hold great potential for future complex water treatment applications.

4. Experimental Section

Further detailed experimental procedures, supporting figures, and tables are provided in Supporting Information.

Supporting Information

Supporting Information is available from the Wiley Online Library or from the author.

Acknowledgements

X.Q. and H.Z. equally contributed to this work. The authors are grateful to the Fundamental Research Funds for the Central Universities (No. FRF-BR-09-021B), 863 (No. 2006AA03Z108) program of China; NSF (DMR-1310266), NIH (R01EB023287) and Harvard Material Research Science and Engineering Center (DMR-1420570) for financial support. H.Z. acknowledges Jane and Aatos Erkko Foundation (4704010), Academy of Finland (decision no. 297580), and Sigrid Juselius Foundation (grant no. 28001830K1) for financial support. H.A.S. acknowledges financial support from the European Research Council (FP/20072013, Grant No. 310892). Cell experiments, AFM, SEM, XPS, DLS, HPLC, and TEM were conducted at the Harvard CNS and FAS centers.

Conflict of Interest

The authors declare no conflict of interest.

Data Availability Statement

The data that support the findings of this study are available in the supplementary material of this article.

Keywords

complex pollutants removal, detergents removal, heavy metals removal, super magnetic response nanocomposites, water treatment

Received: September 30, 2023
Revised: January 23, 2024
Published online:

[1] United Nations, Transforming Our World: the 2030 Agenda for Sustainable Development A/RES/70/1 (UN General Assembly) **2015**.
[2] G. L. Sun, E. E. Reynolds, A. M. Belcher, *Nat. Sustain.* **2020**, *3*, 303.
[3] J. Xu, C. Liu, P.-C. Hsu, J. Zhao, T. Wu, J. Tang, K. Liu, Y. Cui, *Nat. Commun.* **2019**, *10*, 2440.
[4] X. Wan, F. Volpetti, E. Petrova, C. French, S. J. Maerkl, B. Wang, *Nat. Chem. Biol.* **2019**, *15*, 540.
[5] G. A. Engwa, P. U. Ferdinand, F. N. Nwalo, M. N. Unachukwu, *Poisoning in the Modern World-New Tricks for an Old Dog* **2019**, *10*, 70.
[6] D. R. Ortega, D. F. Esquivel, T. B. Ayala, B. Pineda, S. G. Manzo, J. M. Quino, P. C. Mora, V. P. de la Cruz, *Toxics* **2021**, *9*, 23.
[7] G. Genchi, M. S. Sinicropi, G. Lauria, A. Carocci, A. Catalano, *Int J Environ Res Public Health* **2020**, *17*, 3782.
[8] M. S. Chowdhury, X. Zhang, L. Amini, P. Dey, A. K. Singh, A. Faghani, M. Schmueck-Henneresse, R. Haag, *Nano-Micro Lett.* **2021**, *13*, 147.
[9] V. P. Raval, H. H. Desal, *J. Env. Dev.* **2012**, *7*, 851.
[10] N. T. Bui, H. Kang, S. J. Teat, G. M. Su, C.-W. Pao, Y.-S. Liu, E. W. Zaia, J. Guo, J.-L. Chen, K. R. Meihaus, C. Dun, T. M. Mattox, J. R. Long, P. Fiske, R. Kostecki, J. J. Urban, *Nat. Commun.* **2020**, *11*, 3947.
[11] M. Peydayesh, R. Mezzenga, *Nat. Commun.* **2021**, *12*, 3248.
[12] X. Su, A. Kushima, C. Halliday, J. Zhou, J. Li, T. A. Hatton, *Nat. Commun.* **2018**, *9*, 4701.
[13] G. L. Sun, E. E. Reynolds, A. M. Belcher, *Nat. Commun.* **2019**, *10*, 5080.
[14] C. T. Yavuz, J. T. Mayo, W. W. Yu, A. Prakash, J. C. Falkner, S. Yean, L. Cong, H. J. Shipley, A. Kan, M. Tomson, D. Natelson, V. L. Colvin, *Science* **2006**, *314*, 964.
[15] a) T. Ramanathan, A. A. Abdala, S. Stankovich, D. A. Dikin, M. Herrera-Alonso, R. D. Piner, D. H. Adamson, H. C. Schniepp, X. Chen, R. S. Ruoff, S. T. Nguyen, I. A. Aksay, R. K. Prud'Homme, L. C. Brinson, *Nat. Nanotechnol.* **2008**, *3*, 327. b) M. G. Peplow, *Nature* **2013**, *503*, 327; c) S. Stankovich, D. A. Dikin, G. H. Dommett, K. M. Kohlhaas, E. J. Zimney, E. A. Stach, R. D. Piner, S. T. Nguyen, R. S. Ruoff, *Nature* **2006**, *442*, 282.
[16] a) G. M. Scheuermann, L. Rumi, P. Steurer, W. Bannwarth, R. Mulhaupt, *J. Am. Chem. Soc.* **2009**, *131*, 8262; b) R. Romero-Aburto, T. N. Narayanan, Y. Nagaoka, T. Hasumura, T. M. Mitcham, T. Fukuda, P. J. Cox, R. R. Bouchard, T. Maekawa, D. S. Kumar, S. V. Torti, S. A. Mani, P. M. Ajayan, *Adv. Mater.* **2013**, *25*, 5632.
[17] W. Y. Kim, K. S. Kim, *Nat. Nanotechnol.* **2008**, *3*, 408.
[18] W. Zou, Y. Chen, X. Zhang, J. Li, L. Sun, Z. Gui, B. Du, S. Chen, *Carbohydr. Polym.* **2018**, *202*, 246.
[19] Z. Li, X. Zhang, Z. Guo, L. Shi, L. Jin, L. Zhu, X. Cai, J. Zhang, Y. S. Zhang, J. Li, *Mater. Today Adv.* **2021**, *11*, 100150.
[20] H. Shan, Y. Liu, C. Zeng, S. Feng, H. Zhan, *Materials* **2022**, *15*, 7156.
[21] F. Khodabandeloo, S. Shahsavarifar, B. Nayebi, K. P. Niavol, B. Nayebi, R. S. Varma, J. H. Cha, H. W. Jang, D. Kim, M. Shokouhimehr, *Inorg. Chem. Commun.* **2023**, *157*, 111357.
[22] J. Wang, W. S. Cheon, J. Lee, W. Yan, S. Jung, H. Jang, M. Shokouhimehr, *Dalton Trans.* **2023**, *52*, 3567.
[23] B. Qiu, X. Tao, H. Wang, W. Li, X. Ding, H. Chu, *J. Anal. Appl. Pyrolysis* **2021**, *155*, 105081.
[24] B. Qiu, Q. Shao, J. Shi, C. Yang, H. Chu, *Sep. Purif. Technol.* **2022**, *300*, 121925.
[25] H. Zhang, Y. Zhu, L. Qu, H. Wu, H. Kong, Z. Yang, D. Chen, E. Mäkilä, J. Salonen, H. A. Santos, M. Hai, D. A. Weitz, *Nano Lett.* **2018**, *18*, 1448.
[26] F. Kong, H. Zhang, X. Qu, X. Zhang, D. Chen, R. Ding, E. Mäkilä, J. Salonen, H. A. Santos, M. Hai, *Adv. Mater.* **2016**, *25*, 10195.
[27] J. Wu, F. Xu, S. Li, P. Ma, X. Zhang, Q. Liu, R. Fu, D. Wu, *Adv. Mater.* **2019**, *31*, 1802922.
[28] B. Zheng, X. Lin, X. Zhang, D. Wu, K. Matyjaszewski, *Adv. Funct. Mater.* **2020**, *30*, 1907006.
[29] A. Mittal, L. Kurup, J. Mittal, *J. Hazard. Mater.* **2007**, *146*, 243.
[30] Y. Kim, C. Kim, I. Choi, S. Rengaraj, J. Yi, *Environ. Sci. Technol.* **2004**, *38*, 924.
[31] M. Jang, E. W. Shin, J. K. Park, S. I. Choi, *Environ. Sci. Technol.* **2003**, *37*, 5062.